References and Notes

1. H. W. Kroto, J. R. Heath, S. C. O'Brien, R. F. Curl, R. E. Smalley, *Nature* **318**, 162 (1985).
2. S. Iijima, *Nature* **354**, 56 (1991).
3. K. S. Novoselov *et al.*, *Science* **306**, 666 (2004).
4. W. L. Mao *et al.*, *Science* **302**, 425 (2003).
5. Z. W. Wang *et al.*, *Proc. Natl. Acad. Sci. U.S.A.* **101**, 13699 (2004).
6. E. D. Miller, D. C. Nesting, J. V. Badding, *Chem. Mater.* **9**, 18 (1997).
7. M. Wu, X. J. Wu, Y. Pei, Y. Wang, X. C. Zeng, *Chem. Commun.* **47**, 4406 (2011).
8. Y. Iwasa *et al.*, *Science* **264**, 1570 (1994).
9. C. S. Yoo, W. J. Nellis, *Science* **254**, 1489 (1991).
10. M. N. Regueiro, P. Monceau, A. Rassat, P. Bernier, A. Zahab, *Nature* **354**, 289 (1991).
11. B. Sundqvist, *Adv. Phys.* **48**, 1 (1999).
12. F. Moshary *et al.*; de Vries MS, *Phys. Rev. Lett.* **69**, 466 (1992).
13. L. Wang *et al.*, *Appl. Phys. Lett.* **91**, 103112 (2007).
14. L. Marques *et al.*, *Science* **283**, 1720 (1999).
15. M. Núñez-Regueiro, L. Marques, J. L. Hodeau, O. Béthoux, M. Perroux, *Phys. Rev. Lett.* **74**, 278 (1995).
16. M. Barrio *et al.*, *Chem. Mater.* **15**, 288 (2003).
17. F. Michaud *et al.*, *Chem. Mater.* **12**, 3595 (2000).
18. L. Wang *et al.*, *Adv. Mater.* **18**, 1883 (2006).
19. A. Talyzin, U. Jansson, *J. Phys. Chem. B* **104**, 5064 (2000).
20. A. Graja, R. Swietlik, *Synth. Met.* **70**, 1417 (1995).
21. R. Swietlik, P. Byszewski, E. Kowalska, *Chem. Phys. Lett.* **254**, 73 (1996).
22. L. Wang *et al.*, *Chem. Mater.* **18**, 4190 (2006).
23. M. Ramm, P. Luger, D. Zobel, W. Duczek, J. C. A. Boeyens, *Cryst. Res. Technol.* **31**, 43 (1996).

Acknowledgments: We thank H.-k. Mao for valuable comments. We also thank Y. Xiao, G. Shen, S. Yu, V. Prakapenka, A. Kubo, Y. Zhao, W. Cui, R. Liu, and X. Huang for their help. This work was supported as part of EFree, an Energy Frontier Research Center funded by the U.S. Department of Energy (DOE), Office of Science under DE-SC0001057. The use of HPCAT, Advanced Photon Source (APS) is supported by the Carnegie Institute of Washington, Carnegie DOE Alliance Center, University of Nevada at Las Vegas, and Lawrence Livermore National Laboratory through funding from the DOE National Nuclear Security Administration, DOE Basic Energy Sciences, and National Science Foundation (NSF). The use of beamline U2A is supported by NSF (DMR-0805056; EAR 06-49658, Consortium for Materials Properties Research in Earth Sciences (COMPRES)). For the computational research, we used resources from the Oak Ridge Leadership Computing Facility at Oak Ridge National Laboratory, which is supported by the Office of Science of the DOE under contract DE-AC05-00OR22725, and from Holland Computing Center at the University of Nebraska. The synthesis and characterizations of the samples were conducted by the Jilin University group, supported by the National Natural Science Foundation of China (NSFC, 11004072) and Program for New Century Excellent Talents in University (NCET, 2010).

Supplementary Materials

www.sciencemag.org/cgi/content/full/337/6096/825/DC1
Materials and Methods
Supplementary Text
Figs. S1 to S11
References (*24*–*28*)

14 February 2012; accepted 1 June 2012
10.1126/science.1220522

Camouflage and Display for Soft Machines

Stephen A. Morin,[1] Robert F. Shepherd,[1] Sen Wai Kwok,[1] Adam A. Stokes,[1] Alex Nemiroski,[1] George M. Whitesides[1,2]*

Synthetic systems cannot easily mimic the color-changing abilities of animals such as cephalopods. Soft machines—machines fabricated from soft polymers and flexible reinforcing sheets—are rapidly increasing in functionality. This manuscript describes simple microfluidic networks that can change the color, contrast, pattern, apparent shape, luminescence, and surface temperature of soft machines for camouflage and display. The color of these microfluidic networks can be changed simultaneously in the visible and infrared—a capability that organisms do not have. These strategies begin to imitate the functions, although not the anatomies, of color-changing animals.

Cephalopods (such as squid and cuttlefish) have amazing control over their appearance (color, contrast, pattern, and shape) (*1*, *2*). These animals use dynamic body patterns for disguise, for protection, and for warning. Other animals (such as chameleons and many insects) can also actively change their coloration for camouflage or display (*3*, *4*). Still others (such as jellyfish and fireflies) use bioluminescence to communicate (*5*). The color-changing capabilities of these animals have not been replicated by using soft synthetic systems, but such systems could enhance the function of certain machines (such as robots or prosthetics).

This paper describes our initial approaches to change the color, contrast, pattern, apparent shape, luminescence, and infrared (IR) emission (that is, surface temperature) of soft machines fabricated from elastomers and flexible reinforcing sheets (*6*–*8*) by changing the color and pattern of microfluidic networks. These systems are first steps toward imitating the functions, although not the anatomies, of cephalopods (*9*, *10*) and other color-changing animals (*4*). These animals typically change color using specialized cells, such as chromatophores or iridophores (*4*, *9*, *10*), not simple microchannels. The near-perfect matching of environments used by color-changing organisms with highly developed nervous systems is not required for camouflage to be effective.

Nature offers countless examples of camouflage and display (*3*, *11*, *12*). Although specific demonstrations of camouflage vary among species, the strategies used have common themes: background matching, disruptive coloration, and disguise (*3*, *11*, *12*). In background matching, animals use colors and patterns similar to their habitats (*3*, *11*–*13*), such as counter/obliterative shading (for example, rabbits with white underbellies and brown backs) (*11*, *12*). Disruptive coloration breaks up the silhouette of an animal using contrasting patterns that do not follow its shape (*3*). Disguise is a strategy in which an organism adopts the shape and color of objects or animals in the environment (such as stick insects and phasmida) (*3*). Display strategies are used for communication, mating, and hunting and can be just as critical for survival as camouflage (*3*). Bioluminescence is commonly used for display in low- or no-light conditions (*5*, *14*); when lighting is strong, animals sometimes advertise themselves by combining vibrant contrasting colors with distinct shapes (*15*–*17*). For example, jellyfish use bioluminescence to warn would-be predators (*5*), and peacocks use bright plumage to attract mates (*18*).

Although most strategies of camouflage and display (*3*, *12*) emphasize the visible spectrum that most animals (especially mammals) can see (*19*–*21*), there are animals that can see (or otherwise sense) ultraviolet (UV) or IR light and use these spectral regions for signaling or hunting. For example, most birds, many arthropods, and some fish have UV vision (*22*), and many snakes, such as pit vipers, can sense IR light using specialized organs (*23*). Semiconductor technology has expanded our ability to see into the IR (*24*), and we explored techniques for camouflage or display in the IR.

Our system combines microfluidics, pattern, and color to provide both camouflage/display and movement of the soft machines. Camouflage or display results from pumping colored or temperature-controlled fluids through a network of microfluidic channels; mechanical actuation results from pneumatic pressurization and inflation of an independent network of microchannels (pneu-nets) embedded in highly extensible elastomers (*6*, *7*). The microfluidic networks used for camouflage/display are contained in thin silicone sheets [Ecoflex (Smooth-On, Easton, PA), 1 to 2 mm thick] referred to as color layers (Fig. 1 and fig. S1). Although there are technologies, such as electrowetting (*25*) and electrofluidics (*26*), that use microfluidics to tune color, they rely on electric fields to move fluid and are not immediately compatible with our compressed-air power source.

The color layers are easily fabricated (*27*), can cover large areas, and can transport a variety of fluids (both liquids and gases) using similar controls (*28*). The liquids can be colored with dyes or pigments and heated/cooled to change the color of the microfluidic networks in the visible and IR

[1]Department of Chemistry and Chemical Biology, Harvard University, 12 Oxford Street, Cambridge, MA 02138, USA. [2]Wyss Institute for Biologically Inspired Engineering, Harvard University, 60 Oxford Street, Cambridge, MA 02138, USA.

*To whom correspondence should be addressed. E-mail: gwhitesides@gmwgroup.harvard.edu

spectrum; the possible combinations of colorants at different temperatures provide greater flexibility in spectral tailoring than can be achieved by using other technologies: Thermoelectrics can change the IR signature, and electronic displays can change the visible color, but neither technology has control over both IR and visible coloration. Further, once filled, the color layers require no power, have low requirements for volume of fluid (~30 μL/cm^2 of surface), and are lightweight (130 mg/cm^2 of surface). We used closely packed microfluidic channels (Fig. 1) or combined microfluidic channels with wider (millimeters to centimeters) channels (fig. S1D) to create features that are indistinguishable from continuous color in the far field. Ecoflex, unlike the materials used in commercially available flexible electronic displays, has a Young's modulus that is compatible with the flexible bodies and motions of soft machines and is also mechanically robust and inexpensive. The translucency of Ecoflex also helped the machines blend in with their surroundings.

We used a soft robotic quadrupedal "walker" (*7*) to demonstrate that the color layers are light and flexible enough to be compatible with a mobile and stretchy soft machine. We took advantage of the regular and symmetrical shape of the quadruped to illustrate camouflage strategies that can break up recognizable silhouettes.

We attached the color layers to the top of soft quadrupeds (Fig. 1, D to E), which were fabricated as described previously (*6*, *7*). Using a pumping rate of 2.25 mL/min and neglecting the time necessary to fill the tether, a change in color required 30 s (Fig. 1D) [color-change was also monitored with reflectance spectroscopy (fig. S6)]. The weight and flexibility of the color layer did not substantially slow the robot's locomotion (the velocity was 0.6 times the velocity of the same robot without the color layer) (Fig. 1E) (*7*).

Illustrated in Fig. 2 are the operation of camouflage in a rock bed (movie S1) and a leaf-covered concrete slab using two different color layers (Fig. 1 and fig. S1D) filled with two different sets of colored solutions. In all demonstrations, the colored solutions were prepared manually by the operator. Both designs created large, disjointed patches of contrasting brightness similar to the environment but not to the shape of the robot; this disjuncture in shape [disruptive coloration (*3*)] helped conceal the robot. Simple image analysis performed on the camouflaged and uncamouflaged robot (Figs. 2B and 3 and figs. S4 and S5) demonstrated that the brightness of the camouflaged robot was significantly closer to the brightness (within the deviation defined by root mean square contrast) (fig. S4) of the environment than that of the uncamouflaged robot (*27*, *29*). Additionally, we found the similarity in pattern between the background and the camouflaged robot to be favorable (fig. S5). This brightness/contrast resemblance and similarity in pattern was important to this demonstration.

We also investigated the camouflage of soft robots [using background matching (*3*, *11*–*13*)] in a patterned environment similar to a tiled floor (Fig. 2, E to F, and fig. S2) by creating a color layer with periodic microfluidic channels filled with colors matched to that environment. Although not perfectly camouflaged, the colored robots are less obvious and demonstrate the potential of this system. Dynamic camouflage would be useful for applications in which soft machines must do their job without standing out (for example, soft robots performing maintenance operations).

Patterns and contrasting coloration schemes that make the soft machine stand out against a background (display), although less technically demanding than camouflage, are just as important and useful (an example would be to aid location and recovery of soft machines from poorly lit or cluttered environments). We changed the camouflage/display modes of the color layers simply by changing the fluid within them (Fig. 1C, bottom). This ability of a single color layer to switch between modes of coloration is an advantage. We further illustrate display by filling dense, shape-matching color layers (fig. S1B) with fluorescent (Fig. 2, G to H, and movie S2), black and white (Fig. 2J), or chemiluminescent (Fig. 2I and movie S3) solutions that revealed the location of the robots in light or dark.

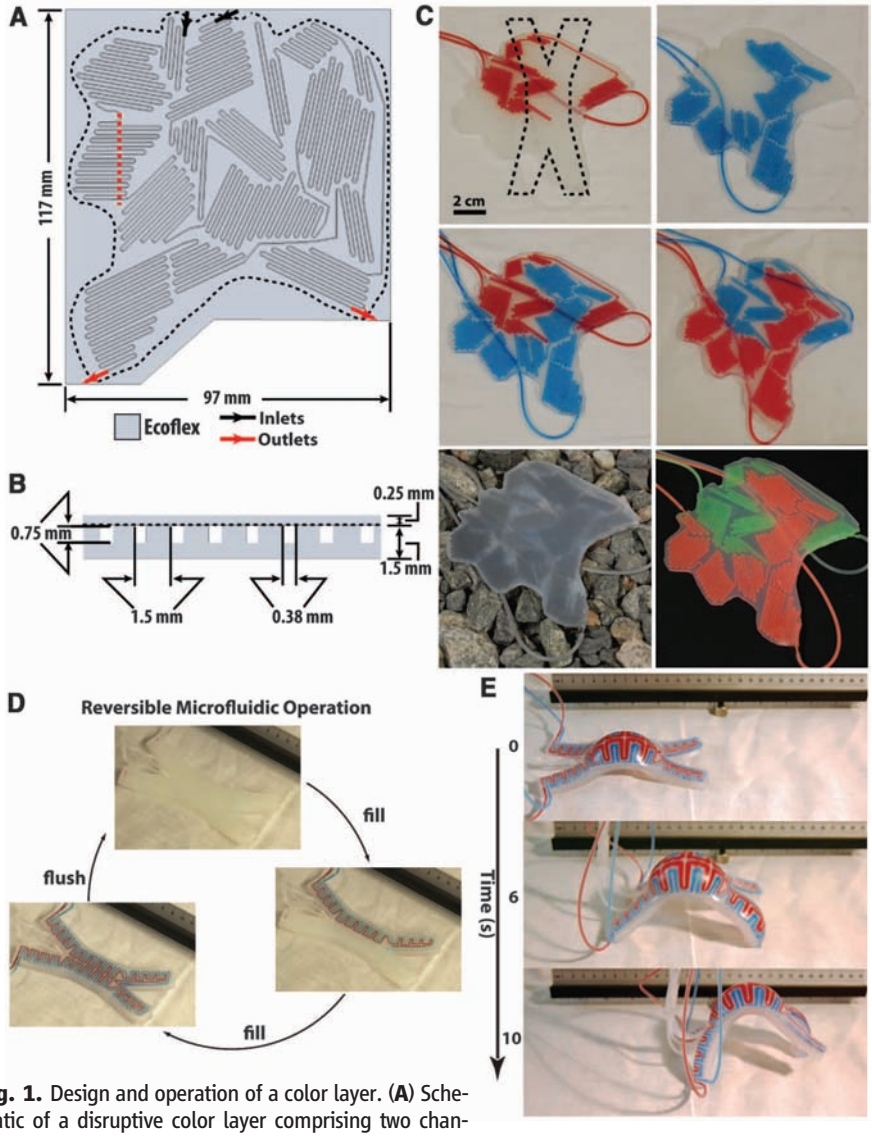

Fig. 1. Design and operation of a color layer. (**A**) Schematic of a disruptive color layer comprising two channels. The dotted black line indicates the final shape. (**B**) Cross-sectional schematic of the region indicated by the dotted red line in (A). (**C**) Various patterns of coloration generated by filling (or not filling) the channels of a completed color layer with solutions of dye (top four images) and pigment dispersions (bottom two images). The dotted line (top left) shows the outline of the quadrupedal soft robot. (**D**) Reversible coloration. This color layer design shows the operation of the system and is not intended to camouflage/display the machine. Colored aqueous solutions are pumped by using a syringe. The pumping rate was 2.25 mL/min (channel volume = 0.75 mL). (**E**) Despite the added weight of a filled color layer, a soft quadruped moves at ~40 m/h (0.6 times the velocity of the same device without the color layer). The major ruler divisions are 1 cm.

We also demonstrated camouflage and display in the IR spectrum (Fig. 4 and movie S4) using warm (70°C) or cool (2°C) colored solutions. Pumping these temperature-controlled solutions through the color layer created contrasting IR color patterns that make the system stand out against its thermal environment. This strategy makes it possible simultaneously to change the visible and IR colors. As an illustration, we camouflaged a color layer within the visible spectrum while simultaneously displaying it in the IR spectrum (Fig. 4, F to G). At a pumping rate of 2.25 mL/min, we achieved IR color change in 80 s (movie S4). The rate of IR color change was limited by the thermal conductivity of Ecoflex [0.16 $Wm^{-1}K^{-1}$ (*27*)] and not the pumping rate.

Simple systems can approach some of the functionality of dynamic coloration that many animals use to control their appearance (*4*). Microfluidic networks that make up a color layer that is

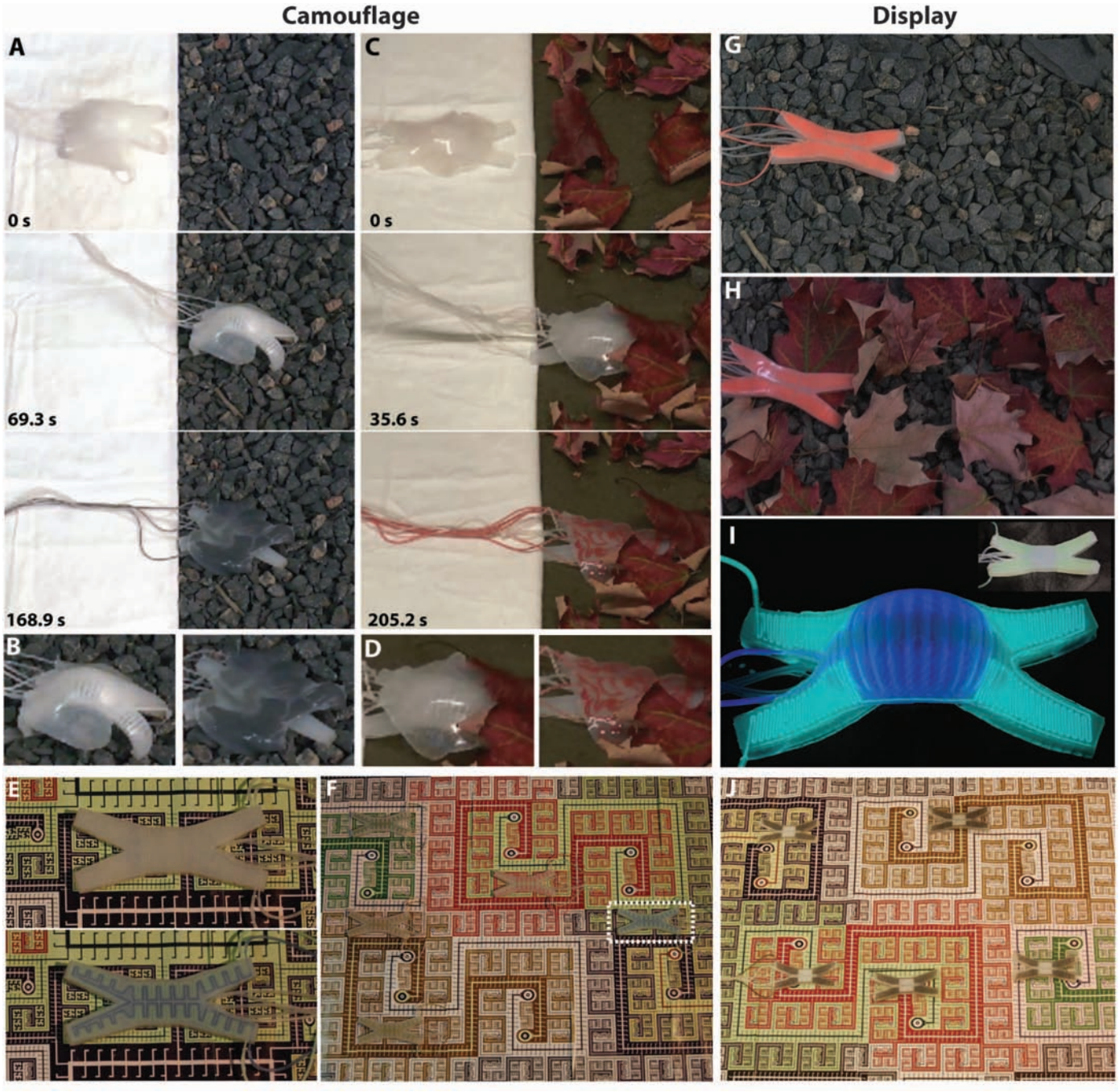

Fig. 2. Camouflage and display coloration. (**A**) Sequential images of a soft robot walking onto a rock bed, where it is camouflaged by pumping colored pigment dispersions through the microfluidic channels in the color layer. The number at the bottom left corner of each frame is the time (seconds). The tether is intentionally left visible to contrast the colors used against a white background. (**B**) Close-up images of the robot uncamouflaged (left) and camouflaged (right). (**C** and **D**) Images of a soft robot walking onto a leaf-covered concrete slab, where it is camouflaged. (**E**) Close-up image of an uncamouflaged (top) soft robot in an artificial, man-made environment and the same soft robot camouflaged (bottom). (**F**) The robot from (E) in five different regions adopting coloration for background matching. One position of the robot from (E) is marked with a dashed box; all five are shown in fig. S3. (**G**) Fluorescent orange robot displayed on a rock bed. (**H**) Robot from (G) displayed on a leaf-covered rock bed. (**I**) Robot glowing in the dark using chemiluminescence. (Inset) The same robot photographed in the light. (**J**) Robots displayed in contrasting black and white on the pattern from (F). All quadrupeds were 13 cm long (Fig. 1).

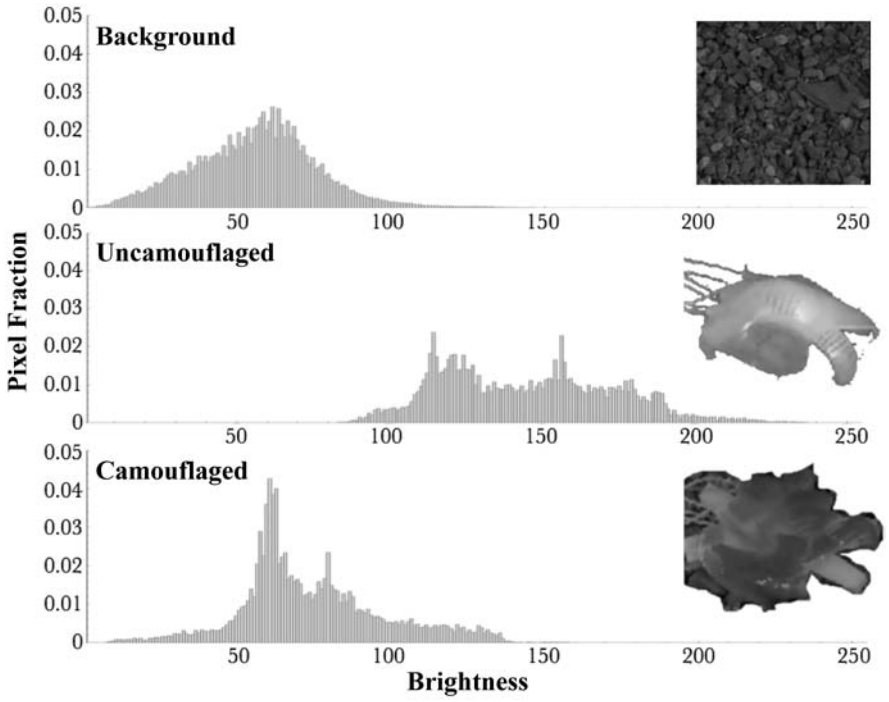

Fig. 3. Stacked histograms showing the distribution of gray-scale intensities (brightness) generated by image analysis of a rocky environment (background), an isolated uncamouflaged soft robot, and an isolated camouflaged soft robot. (Insets) The analyzed images.

independent of other functions can effectively—albeit crudely when compared with animals—camouflage or display soft machines by altering their apparent shape, color, contrast, luminescence, temperature, and pattern. The ability of color layers simultaneously to change color in the visible and the IR is a capability not used by organisms and not easily replicated by using other technologies: Animals are limited in their ability to control their temperature; soft machines fabricated in silicone elastomers are not.

These devices confirm that microfluidic channels can serve multiple functions in soft machines: actuation, camouflage, display, fluid transport, and temperature regulation. Combining different functional microfluidic systems simplifies the design and increases the functionality of soft machines. Complex/specialized microfluidic networks can take the place of these relatively simple color layers to bring more capabilities (such as reagent handling and storage) to soft machines.

We believe that the simple design, fabrication, and operation of these color-changing soft machines make these systems accessible and potentially useful to many different scientific fields. Biologists studying camouflage/display could use specially designed soft machines to observe how dynamic color, temperature, and pattern influence

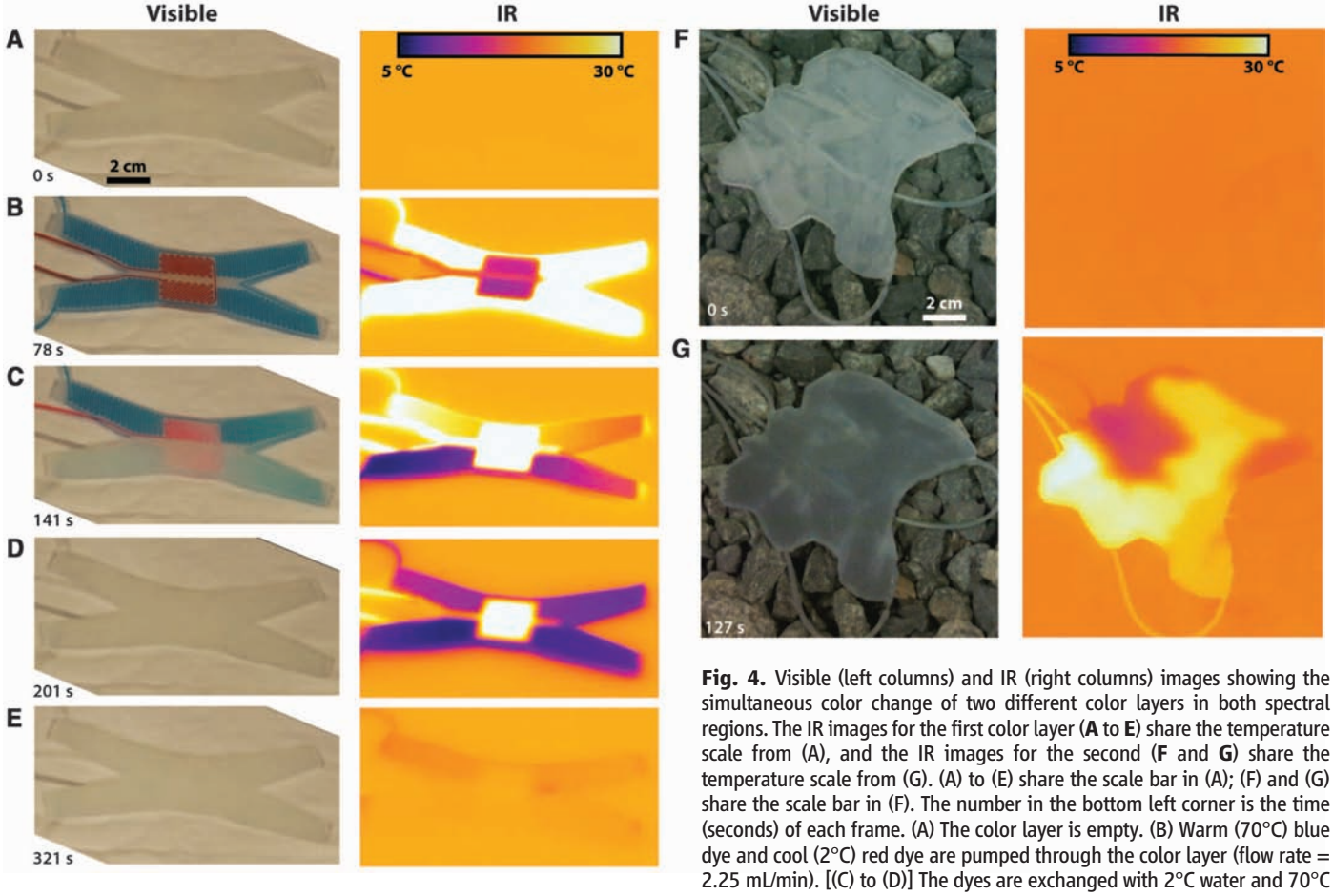

Fig. 4. Visible (left columns) and IR (right columns) images showing the simultaneous color change of two different color layers in both spectral regions. The IR images for the first color layer (**A** to **E**) share the temperature scale from (A), and the IR images for the second (**F** and **G**) share the temperature scale from (G). (A) to (E) share the scale bar in (A); (F) and (G) share the scale bar in (F). The number in the bottom left corner is the time (seconds) of each frame. (A) The color layer is empty. (B) Warm (70°C) blue dye and cool (2°C) red dye are pumped through the color layer (flow rate = 2.25 mL/min). [(C) to (D)] The dyes are exchanged with 2°C water and 70°C water. (E) Room temperature (22°C) water is pumped into both channels. (F) An unfilled color layer is seen in the visible but camouflaged in the IR. (G) The color layer from (F) is camouflaged in the visible by using two shades of gray pigment dispersions. One dispersion is at 70°C, and the other is at 2°C.

animal behavior (such as predator/prey relationships) (*13*, *30*). In anatomy, our devices could simulate fluid vessels and muscle motion for realistic modeling or training. Although we have focused on soft robots, our display systems can also interface with hard robots and present new opportunities for modifying the appearance of these devices. These applications are approachable by using tethered microfluidic systems such as those demonstrated here, but some applications will demand more technically advanced autonomous systems. The challenges associated with autonomy will be addressed initially by using larger-bodied machines or robots that can carry power sources, pumps, electronics, and fluids.

References and Notes

1. R. T. Hanlon, *Curr. Biol.* **17**, R400 (2007).
2. R. T. Hanlon *et al.*, *Philos. Trans. R. Soc. B Biol. Sci.* **364**, 429 (2009).
3. H. B. Cott, *Adaptive Coloration in Animals* (Methuen, London, 1957).
4. D. Stuart-Fox, A. Moussalli, *Philos. Trans. R. Soc. B Biol. Sci.* **364**, 463 (2009).
5. J. W. Hastings, *J. Mol. Evol.* **19**, 309 (1983).
6. F. Ilievski, A. D. Mazzeo, R. F. Shepherd, X. Chin, G. M. Whitesides, *Angew. Chem. Int. Ed.* **50**, 1890 (2011).
7. R. F. Shepherd *et al.*, *Proc. Natl. Acad. Sci. U.S.A.* **108**, 20400 (2011).
8. R. V. Martinez, C. R. Fish, X. Chen, G. M. Whitesides, *Adv. Funct. Mater.* **22**, 1376 (2012).
9. L. M. Mäthger, R. T. Hanlon, *Cell Tissue Res.* **329**, 179 (2007).
10. R. L. Sutherland, L. M. Mäthger, R. T. Hanlon, A. M. Urbas, M. O. Stone, *J. Opt. Soc. Am. A Opt. Image Sci. Vis.* **25**, 588 (2008).
11. G. H. Thayer, A. H. Thayer, *Concealing-Coloration in the Animal Kingdom: An Exposition of the Laws of Disguise Through Color and Pattern: Being a Summary of Abbott H. Thayer's Discoveries* (Macmillan, New York, 1909).
12. M. Stevens, S. Merilaita, *Philos. Trans. R. Soc. B Biol. Sci.* **364**, 423 (2009).
13. S. Merilaita, J. Lind, *Proc. R. Soc. London B Biol. Sci.* **272**, 665 (2005).
14. T. Wilson, J. W. Hastings, *Annu. Rev. Cell Dev. Biol.* **14**, 197 (1998).
15. K. V. Langridge, *Anim. Behav.* **77**, 847 (2009).
16. M. D. Norman, J. Finn, T. Tregenza, *Proc. R. Soc. London B Biol. Sci.* **266**, 1347 (1999).
17. E. Scholes III, *Biol. J. Linn. Soc. London* **94**, 491 (2008).
18. M. Petrie, T. Halliday, C. Sanders, *Anim. Behav.* **41**, 323 (1991).
19. G. H. Jacobs, *Biol. Rev. Camb. Philos.* **68**, 413 (1993).
20. T. H. Goldsmith, *Q. Rev. Biol.* **65**, 281 (1990).
21. D. G. Luo, W. W. S. Yue, P. Ala-Laurila, K. W. Yau, *Science* **332**, 1307 (2011).
22. D. M. Hunt, S. E. Wilkie, J. K. Bowmaker, S. Poopalasundaram, *Cell. Mol. Life Sci.* **58**, 1583 (2001).
23. R. C. Goris, *J. Herpetol.* **45**, 2 (2011).
24. A. Rogalski, *Prog. Quantum Electron.* **27**, 59 (2003).
25. R. A. Hayes, B. J. Feenstra, *Nature* **425**, 383 (2003).
26. J. Heikenfeld *et al.*, *Nat. Photonics* **3**, 292 (2009).
27. Materials and methods are available as supplementary materials on *Science* Online.
28. G. M. Whitesides, *Nature* **442**, 368 (2006).
29. J. A. Endler, *Biol. J. Linn. Soc. London* **41**, 315 (1990).
30. I. C. Cuthill *et al.*, *Nature* **434**, 72 (2005).

Acknowledgments: The development of biomimetic camouflage strategies was supported by the U.S. Department of Energy under award DE-FG02-00ER45852. Soft machine development was supported by the Defense Advanced Research Projects Agency under award W911NF-11-1-0094. Patent applications "Flexible Robotic Actuators" and "Soft Robotic Actuators" have been filed but not yet published.

Supplementary Materials

www.sciencemag.org/cgi/content/full/337/6096/828/DC1
Materials and Methods
Supplementary Text
Figs. S1 to S6
References (*31*–*35*)
Movies S1 to S4

20 March 2012; accepted 4 June 2012
10.1126/science.1222149

Mixed-Phase Oxide Catalyst Based on Mn-Mullite (Sm, Gd)Mn_2O_5 for NO Oxidation in Diesel Exhaust

Weichao Wang,[1*]† Geoffrey McCool,[1]† Neeti Kapur,[1] Guang Yuan,[1] Bin Shan,[1,2] Matt Nguyen,[1] Uschi M. Graham,[3] Burtron H. Davis,[3] Gary Jacobs,[3] Kyeongjae Cho,[1,4,5*] Xianghong (Kelly) Hao[1*]

Oxidation of nitric oxide (NO) for subsequent efficient reduction in selective catalytic reduction or lean NO_x trap devices continues to be a challenge in diesel engines because of the low efficiency and high cost of the currently used platinum (Pt)–based catalysts. We show that mixed-phase oxide materials based on Mn-mullite (Sm, Gd)Mn_2O_5 are an efficient substitute for the current commercial Pt-based catalysts. Under laboratory-simulated diesel exhaust conditions, this mixed-phase oxide material was superior to Pt in terms of cost, thermal durability, and catalytic activity for NO oxidation. This oxide material is active at temperatures as low as 120°C with conversion maxima of ~45% higher than that achieved with Pt. Density functional theory and diffuse reflectance infrared Fourier transform spectroscopy provide insights into the NO-to-NO_2 reaction mechanism on catalytically active Mn-Mn sites via the intermediate nitrate species.

Diesel engines are attractive because of their higher fuel efficiency than gasoline engines (*1*). However, their lean exhaust with high oxygen (O_2) content requires specialized devices to reduce the engine-generated nitrogen oxide (NO_x) pollutants, mostly nitric oxide (NO), to environmentally benign nitrogen (N_2). One popular strategy is the use of selective catalytic reduction (SCR) of NO_x with ammonia (NH_3) through the reaction: $2NH_3 + NO + NO_2 \rightarrow 2N_2 + 3H_2O$. The rate of this reaction is maximized (fast SCR) when the NO:NO_2 ratio approaches unity (*2*, *3*). A lean NO_x trap (LNT) adsorbs NO_x under lean conditions and reduces NO_x to N_2 under fuel-rich regeneration cycles. NO oxidation products such as nitrogen dioxide (NO_2) have a higher trapping efficiency on LNT materials (*4*). In addition to the NO_x-based pollutants, diesel engines also generate black soot with polynuclear aromatic content. One process to remove carbon soot is a continuous regenerable trap (CRT), which uses NO_2 as an oxidant ($2NO_2 + C \rightarrow CO_2 + 2NO$, $NO_2 + C \rightarrow CO + NO$). Oxidation of engine-generated NO to NO_2 is critical in diesel engine emission control for reducing NO_x and carbon soot from the tail-pipe exhaust.

To date, no thermally stable material has matched platinum's catalytic performance under diesel exhaust temperatures, despite a substantial amount of work that has been undertaken in search for catalysts based on metal oxides (*5*, *6*). Here, we report a class of hydrothermally stable, mixed-phase oxides based on Mn-mullite, (Sm, Gd)Mn_2O_5. This catalyst demonstrates activity at temperatures as low as 120°C and has a ~64% increase in NO oxidation catalytic performance over 2% Pt on γ-Al_2O_3 at 300°C. The catalytic behavior is mainly linked to the Mn-Mn dimers on the mullite surface based on characterization methods and quantum-mechanical simulations.

Mixed-phase oxide catalysts were prepared by a coprecipitation method (*7*). Transition metal, alkaline earth, and rare earth precursors were dissolved in water with a non-ionic surfactant. The pH was adjusted to between 9 and 10 with tetramethylammonium hydroxide, followed by the addition of oxalic acid and hydrogen peroxide. The precipitate was filtered, dried, calcined, and hydrothermally aged (materials and methods S-I).

To evaluate catalytic performance, we exposed the aged sample $Mn_7CeSmSrO_{14.83}$, labeled MnCe-7:1, to the reactant gas mixture (450 parts per million NO and 10% O_2) while ramping the temperature up to 350°C to test for NO conversion (materials and methods S-II).

[1]Nanostellar Inc., 3696 Haven Avenue, Redwood City, CA94063, USA. [2]State Key Laboratory of Materials Processing and Die and Mould Technology and School of Materials Science and Engineering, Huazhong University of Science and Technology, Wuhan 430074, Hubei, China. [3]Center for Applied Energy Research, University of Kentucky, 2540 Research Park Drive, Lexington, KY 40511, USA. [4]Department of Materials Science and Engineering and Department of Physics, University of Texas at Dallas, Richardson, TX 75080, USA. [5]WCU Multiscale Mechanical Design Division, School of Mechanical and Aerospace Engineering, Seoul National University, Seoul 151-742, Republic of Korea.

*To whom correspondence should be addressed. E-mail: wwang@nanostellar.com (W.W.); kjcho@utdallas.edu (K.C.); xhao@nanostellar.com (X.H.)
†These authors contributed equally to this work.